AIChE

Systematic Controllability Analysis for Chemical Processes

Zhihong Yuan, Nan Zhang, Bingzhen Chen, and Jinsong Zhao
Dept. of Chemical Engineering, Tsinghua University, Beijing, China

DOI 10.1002/aic.13722
Published online January 17, 2012 in Wiley Online Library (wileyonlinelibrary.com).

Modern chemical industrial processes are becoming more and more integrated and consist of multiple interconnected nonlinear process units. These strong interactions profoundly complicate a system's inherent properties and further alter the plant-wide process dynamics. This may lead to a poor control performance and cause plant-wide operability problems. To ensure entire processes run robustly and safely, with considerable profitability, it is crucial to recognize the inherent characteristics that can jeopardize controllability and process behavior at the early design stage. With a focus on inherently safer designs, from a plant-wide perspective, a systematic method for chemical processes controllability analysis is addressed in this study. In the proposed framework, based on open-loop stability/instability and minimum/nonminimum-phase behavior, the entire operating zone of the process can be categorized into distinct subregions with different inherent properties. Variations in the inherent characteristics of a plant-wide process with the operation and design conditions, over the feasible operation region, can be probed and analyzed. An attempt of this framework is made to illustrate how to clarify the roots of the poor controllability that arise in the design and operation of a large scale chemical process, and the results can provide guidance for both deciding the optimal operation conditions and selecting the most suitable control structure. Singularity theory is also applied in the framework to improve the computational efficiency. The framework is illustrated with two case studies. One involves a reactor-external heat exchanger network and the other a more complex plant-wide process, comprising a reactor, an extractor, and a distillation column. © 2012 American Institute of Chemical Engineers *AIChE J,* 58: 3096–3109, 2012

Keywords: chemical processes, controllability, stability, phase behavior, singularity

Introduction

Modern chemical processes are becoming increasingly integrated and have more interactions between various process units to reduce capital and operating costs. The interactions between these units, including recycle and bypass streams, typically intensify the complexity and nonlinearity of large-scale plant-wide processes. Numerous studies have demonstrated that the presence of nonlinearities, including input/output multiplicities and oscillatory and chaotic behavior, can cause control challenges.[1–4] A traditional sequential design approach may lead to serious operating difficulties. Therefore, systematic strategies that consider the nonlinearities have been needed to improve the designs and controllability of chemical processes that exhibit undesirable inherent characteristics.

Having a consistently stable chemical process is a prerequisite for ensuring safe production. Stability and controllability are two important inherent characteristics for a process, in terms of its operability.[5] Many chemical systems exhibit input/output multiplicity characteristics and nonminimum-phase behavior, and these inherent characteristics are known to impose limitations on process operation and control performance, regardless of what control algorithms are implemented. As process design fundamentally determines these inherent properties, and analyzing the influences of these limitations early enough can allow timely modifications to ameliorate or avoid these characteristics, it is useful to gather information about these characteristics at the early design stage of the entire chemical process.

Over the past few decades, the field of stability and controllability analysis for single chemical unit has matured considerably, with a large number of valuable reports being published. Research efforts have been focused on the nonlinear phenomena known to generate operability difficulties, such as multiple equilibrium points, limit cycles, chaotic behavior, and bifurcations, for example, Refs. 6–12. Flores-Tlacuahuac and coworkers[13–16] addressed the effects of potential manipulated, disturbance, and design variables on the nonlinearity and stability of the polymerization reactors. Hernjak et al.[17] presented a qualitative process operability analysis method involving three primary process characteristics: the degree of nonlinearity, the process dynamics and the degrees of interaction between the loops. Kienle and coworkers[18,19] analyzed the behavior of different coupled reactor–separator systems using bifurcation theory. Bildea and coworkers[20,21] investigated the multiplicity behavior of six reaction systems for the continuous stirred tank reactor (CSTR)–separator–recycle polymerization systems. Compared with bifurcation and nonlinearity analysis, there is an extensive literature regarding controllability analysis. There are numerous ways to define and assess the controllability of a process.[22] Research has also shown that performing a detailed bifurcation and stability

Correspondence concerning this article should be addressed to B. Chen at dcecbz@tsinghua.edu.cn.

analysis more routinely in a process design would improve controllability, and could prove helpful for developing and implementing model-based controllers for nonlinear chemical processes.[23–25] Ma and Bogle[26] have proposed an approach using continuation and optimization methods, which aid in the modification of a process design to avoid control difficulties due to input multiplicity. Yuan et al.[27] has formulated a method to segregate the entire operating region of a single chemical reactor into several subregions, in consideration of both stability and phase behavior simultaneously. A large number of contributions regarding plant-wide controllability analysis have been published,[28–38] mainly focusing on the interactions between control loops, the determination of variable pairing (the selection of controlled and manipulated variables) and the effects of recycles and energy integrations at certain operating points. Recently, Rojas et al.[39] has developed an operability analysis approach for nonlinear plant-wide processes from a network perspective based on dissipativity. However, until now, few papers have addressed the analysis of nonlinearity and controllability for complex chemical plant-wide processes over the entire feasible operating region.

From the viewpoint of control, once the dynamics are known, advanced control algorithms would allow one to deal with almost any difficult control situation. Feedback interactions between the units of a plant-wide process, typically give rise to more complex network dynamics. To keep plant-wide processes running stable and safely with considerable profitability, different plant-wide control architectures have been proposed. These approaches fall into four main categories:[40] decentralized,[41–43] distributed,[44–48] multilayer,[49–51] and single layer.[52–54] The advantages and disadvantages of these four plant-wide control architectures were summarized by Ochoa.[55] Plant-wide control problems in chemical and biochemical processes remain an important problem for both academia and industry. Although many control strategies have been fixed successfully for several processes, the operation settings rarely remain fixed at their design settings. When a disturbance enters the process, the characteristics of the current operating point may change, so it is necessary to understand the relationship between the inherent characteristics and operating/design conditions. Conversely, each single unit having stable and good controllability properties does not guarantee the same for the ultimately formed network. Therefore, it is of critical importance to analyze the operability problems from the network perspectives. In addition, modifications to a process design itself, such as to the values of operating/design parameters or topology structure, can sometimes affect the dynamics of the process more than adjusts in the controllers.[56] As such, it is important to ascertain the open-loop controllability of the chemical process and to identify how the inherent properties vary with the process design/operation from the plant-wide perspective. Luyben has investigated a subtle phenomenon with recycle streams, the snowball effect, which is characterized by a large sensitivity of one or more of the variables in a recycle loop to small changes in a disturbance variable.[57,58] Existing research also has shown that a control structure that fixes the flow rate of one stream somewhere in a liquid recycle loop can prevent the snowball.[57] Extended bifurcation diagrams[59] can facilitate changes to the process network design, to ameliorate some of the instability and poor controllability introduced by large recycle streams and/or heat integration schemes.

In consideration of the above, by understanding the phase behavior and open-loop stability for plant-wide processes, from the network perspective, based on the nonlinear plant-wide process model, we can develop a systematic framework that can identify potential control problems associated with the inherent characteristics of a plant-wide process over the entire feasible operating region. In this framework, phase behavior is selected as an indicator of open-loop controllability. The phase behavior (minimum/nonminimum-phase behavior) and open-loop stabilities of a process, as well as their relationships with the process design and operation, can provide valuable guidance for both process design modifications and plant-wide process control system design. The article is structured as follows. Initially, the problems that need to be addressed are outlined with a series of reactor networks. Then, the development of the systematic methodology for the plant-wide process controllability analysis is discussed. The presented framework is then illustrated with two case studies. The first involves a reactor-external heat exchanger network and the second a more complex chemical process with several recycles, consisting of a reactor, an extractor, and a distillation column. Finally, the main conclusions from the work are discussed.

Problem Statement

The following network[44] involves two reactors in series, as shown in Figure 1, where three irreversible elementary exothermic reactions ($A \xrightarrow{k_1} B$, $A \xrightarrow{k_2} U$, $A \xrightarrow{k_3} R$) occur in parallel, A is the reactant species, B is the desired product, U and R are the undesired byproducts. The reactors are connecting by F_1 and F_r. The above process is taken as an illustrative example to formulate the problem that will be solved in this work.

The overall nonlinearity and internal dynamic behavior of chemical processing plants, with material recycling, can be substantially different from those in the individual processing units. Our previous preliminary research work has allowed the steady-state solution diagrams for the above reactors to be devised.[60] Based on the values of the process parameters which can be found elsewhere,[44,60] Figure 2 presents the steady-state map for both the entire system and the single reactor, respectively. The differences in shape between the steady-state solution curves for the plant-wide process and single unit are significant, and the entire system exhibits input and output multiplicity simultaneously. The steady-state behavior for the single reactor is relatively simple, and only the output multiplicity exists. Material recycling dramatically alters the shape of the steady-state map for the process and gives rise to instability, even when the individual processing units are stable.

From a control theory point of view, F_r represents a positive feedback that would cause closed-loop instability and control difficulties. Moreover, in the desirable conversion subregion, plant interconnections alter the gain and time constants and further introduce nonminimum-phase behavior, leading to poor controllability. They also impose fundamental limitations on the achievable performance of conventional control systems.

In reality, the connections between the various single units in the plant-wide process are more complex than those presented in the illustrated example above. It is not only the material/energy recycles but also disturbances such as in inlet temperature and feed flow rate, that may affect the

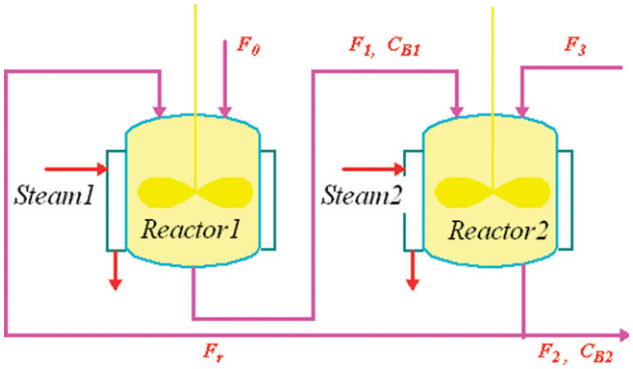

Figure 1. Process flow sheet of the illustrative example.

[Color figure can be viewed in the online issue, which is available at wileyonlinelibrary.com.]

overall nonlinearity of the network. Therefore, this study will investigate the internal characteristics of the overall networks that are widespread in chemical processes, and address the follow three questions:

Question 1. *How can processes be well controlled or is it difficult to control a process that is operated at, or near, the point that provides high profitability?*

Question 2. *How does the stability and phase behavior vary with process design and operation?*

Question 3. *How can a plant-wide process with poor controllability be redesigned?*

For a plant-wide process, like the illustrated process described in Figure 1, there are many variables that need to be controlled. The majority of them, such as temperature, may be controlled locally.[61] However, even when each single controller is well fixed at the operating point, one cannot guarantee that the overall network will work well. Material balances in general, and the material balances of impurities especially, are established by considering the interactions between the different operating units and recycle loops. Therefore, controllability and stability analysis requires a plant-wide approach. It should be noted that we will consider the control-affine systems, as shown in Eq. 1, in the subsequent discussions in this article.

$$\begin{aligned} \dot{x} &= f(x) + g(x)u \\ y &= h(x) \end{aligned} \tag{1}$$

where $x = [x_1, x_2, ..., x_n] \in R^n$ denotes the n vector of state variables, u denotes the manipulated input, $y = [y_1, y_2, ..., y_m] \in R^m$ denotes the m vector of controlled outputs, $f(x)$ and $g(x)$ are smooth vector functions from R^n to R^n and $h(x)$ is a smooth scalar function of R^n.

Methodology Development

For the three questions listed in the previous section that need to be satisfied, the framework of the proposed systematic methodology is presented in Figure 3.

F is a vector of residuals of the steady-state equations for the entire process and J_F denotes the Jacobian matrix of F. Rank (J_F) determines whether the operating point is a singularity point or not. F_{zd} represents the vector of residuals of the zero dynamics equations. $J_{F_{zd}}$ represents the Jacobian matrix of F_{zd}. The basis of the presented approach is to explore the steady-state maps between the manipulated and controlled variables of the plant-wide process, in such a way, that the influences of any operations on the nonlinearities become apparent.

Remark 1. *Set* $\alpha = n - \sum_{i=1}^{m} r_i$, $\eta = [\eta_1, \eta_2, ..., \eta_\alpha] \in R^\alpha$ *denotes the* α*-vector of state variables of the zero dynamics. For a nonlinear multiinput, multioutput plant-wide process as described by Eq.* 1. r_i*, the relative order of output* y_i $(i = 1, 2, ..., m)$ *with respect to the manipulated input* u*. The relative order of the process will determine the number of expressions for the zero dynamics. If* $\alpha = 0$*, the plant-wide process has no zero dynamics;*[62] *otherwise, the system contains* α *zero dynamics. The detailed algorithm for obtaining the zero dynamics from the normal form is described in Ref.* 63*, and is extended in this article to solve the zero dynamics for the entire chemical process.*

A step by step description of the methodology for analyzing the controllability of a plant-wide process shown in Figure 3 is outlined as follows:

Step 1. *Obtain the steady-state maps between the manipulated and controlled variables.*

Step 2. *This step involves the following substeps*:

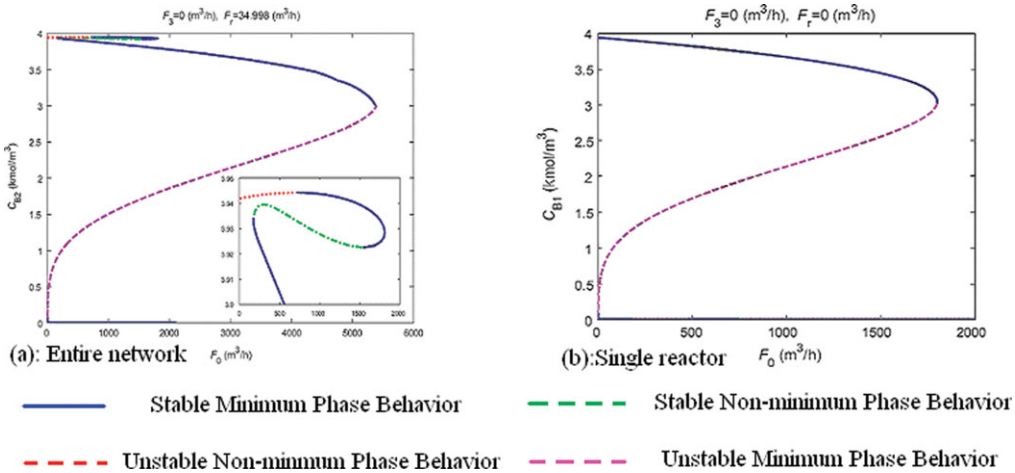

Figure 2. Steady-state solution diagrams for the illustrative example (—stable steady-state solutions, ----unstable steady-state solutions).

[Color figure can be viewed in the online issue, which is available at wileyonlinelibrary.com.]

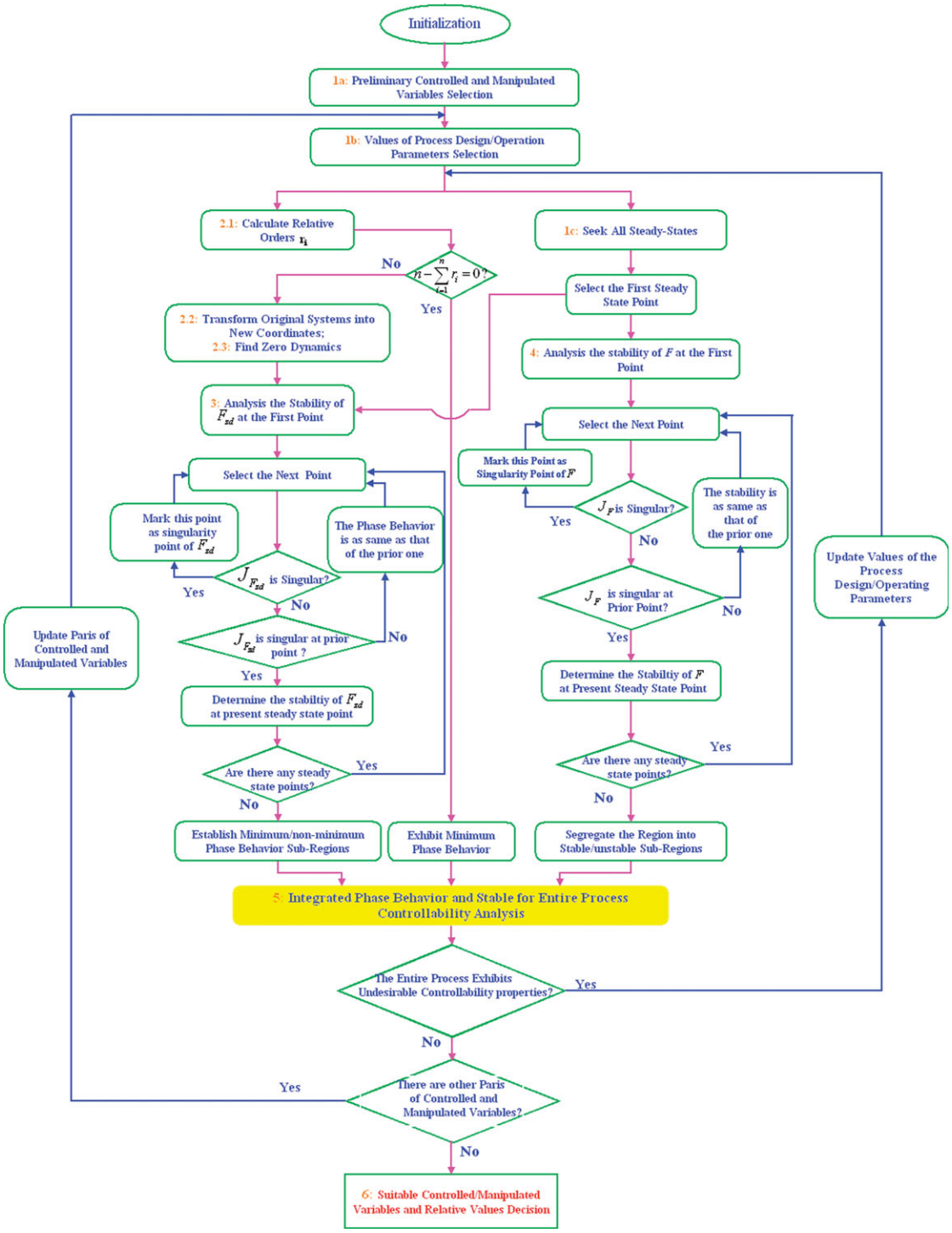

Figure 3. Schematic representation of the proposed methodology for plant-wide process.

[Color figure can be viewed in the online issue, which is available at wileyonlinelibrary.com.]

Step 2.1. *Calculate the relative order,* r_i (i=1, 2,…m), *of the entire chemical process*;

Step 2.2. *Transform the original nonlinear system into new coordinates;*

Step 2.3. *Extract the expression for the zero dynamics.*

Step 3. *This step involves phase behavior analysis over the whole feasible operating region, and can be divided into three substeps*:

Step 3.1: *Calculate* Jacobian *matrix* $J_{F_{zd}}$ *for the zero dynamics.*

$$J_{F_{zd}} = \begin{bmatrix} \frac{\partial(dF_{zd_1}/dt)}{\partial F_{zd_1}} & \frac{\partial(dF_{zd_1}/dt)}{\partial F_{zd_2}} & \cdots & \frac{\partial(dF_{zd_1}/dt)}{\partial F_{zd_\alpha}} \\ \frac{\partial(dF_{zd_2}/dt)}{\partial F_{zd_1}} & \frac{\partial(dF_{zd_2}/dt)}{\partial F_{zd_2}} & \cdots & \frac{\partial(dF_{zd_2}/dt)}{\partial F_{zd_\alpha}} \\ \cdots & \cdots & \cdots & \cdots \\ \frac{\partial(dF_{zd_\alpha}/dt)}{\partial F_{zd_1}} & \frac{\partial(dF_{zd_\alpha}/dt)}{\partial F_{zd_2}} & \cdots & \frac{\partial(dF_{zd_\alpha}/dt)}{\partial F_{zd_\alpha}} \end{bmatrix} \quad (2)$$

$$\alpha = n - \sum_{i=1}^{m} r_i \quad (3)$$

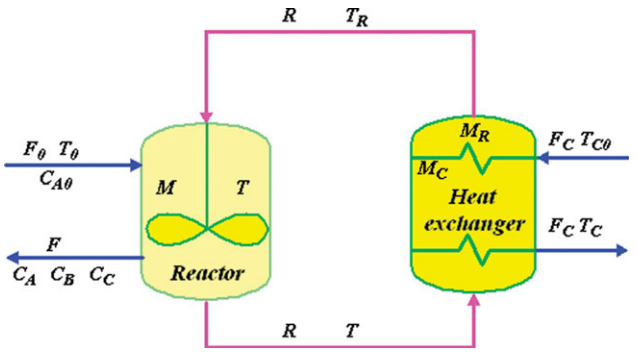

Figure 4. Reactor with external heat exchanger networks.

[Color figure can be viewed in the online issue, which is available at wileyonlinelibrary.com.]

Step 3.2. *Find the singularity point for the zero dynamics. If* $\mathrm{Rank}(J_{F_{zd}})<\alpha$ *at a certain steady state, then this steady-state point is a singularity point of zero dynamics. The entire operating region can be segregated into several suboperating regions by the singularity points.*

Step 3.3. *Check the stability status of the zero dynamics. Stable zero dynamics indicate that the original plant-wide process, from which the zero dynamics are extracted, exhibits minimum-phase behavior. Otherwise, the process has nonminimum-phase behavior.*

Step 4. *Stability analysis for the plant-wide process. The procedure here is similar to that in Step 3. It involves obtaining the original system's singularity points and analyzing the stability status of the plant-wide process to each side of the singularity points.*

Step 5. *Controllability analysis, based on the results obtained from the above two steps. The entire operating region can be divided into several subregions, which have a different phase behavior and stability status.*

Step 6. *Desirable controlled/manipulated variables and related values decision. In other words, select the pairs of controlled/manipulated variables to determine whether they have a significant influence on reducing the size of the open-loop unstable and nonminimum-phase regions.*

Remark 2. *As the phase behavior may change when a process crosses the zero dynamics' singularity points, it is necessary to only select one steady-state operating point to each side of the singularity points to check the stability status. It is not necessary to investigate the stability of the zero dynamics at all of the steady-state points.*

Remark 3. *Based on the phase behavior (minimum-phase behavior and nonminimum-phase behavior), the controllability analysis for a single unit is discussed in previous work.*[27,59] *By integrating the open-loop stability and phase behavior analysis in the process design, the operating region of the whole process can be divided into four regions: The stable-minimum-phase behavior (S-MP) subregion; the stable-nonminimum-phase behavior (S-NMP) subregion; the unstable-minimum-phase behavior (US-MP) subregion; and the unstable-nonminimum-phase behavior (US-NMP) subregion. This segregation strategy is also applied in the plant-wide process controllability analysis.*

These six steps make up the proposed methodology for the controllability analysis of a plant-wide process. The presented framework will be applied to two plant-wide processes to demonstrate its efficiency.

Case Studies for Plant-Wide Process Controllability Analysis

Two case studies have been selected in this section, to illustrate the presented methodology. The first case study deals with a reactor-external heat exchanger network, and the second involves a more complex plant-wide process, comprising a reactor, an extractor, and a distillation column.

Case study I: reactor-external heat exchanger network

Process Introduction. For many industrial chemical processes, direct heating/cooling in isothermal operations is often impractical or unfeasible. In such instances, large material recycle streams are adapted where the heat carries, by connecting the reaction unit to an external heat exchanges system.[64] This system can be used in both batch and continuous processes, and is quite common in processes featuring fast, highly exothermic reactions, such as in gas-phase ethylene polymerization processes.[65] There are three advantages to this configuration. First, it allows for a higher-energy flow through the entire network to improve the efficient of the heat exchange. Second, it affords the process designer flexibility in terms of heat-transfer area that is independent of the reactor geometry. Third, the efficiency of the external heat exchanger can be improved by increasing the heat capacity of the recycle stream, either by using an excess quantity of a reactant or by introducing an inert diluent into the recycle loop, along with a separation unit.[66] However, a process with this configuration has a high degree of nonlinearity and requires a complex control system design.[67,68] In this subsection, the nonlinearity and the internal characteristics of the reactor-external heat exchanger network will be investigated.

This case study, considers a process network comprising a reactor and a heat exchanger as shown in Figure 4. The process involves two consecutive, highly exothermic reactions, $A \xrightarrow{k_1} B \xrightarrow{k_2} C$, with pre-exponential factors k_{10} and k_{20}, activation energies E_{a_1} and E_{a_2}, and heats of reaction ΔH_1 and ΔH_2, respectively. The heat of reaction is removed via an external heat exchanger.[69] M denotes the reactor holdup, M_R denotes the holdup in the tube side of the heat exchanger, M_c denotes the holdup in the shell side, F_0 denotes the feed rate into the reactor, A represents the reactants and C_{A_0} denotes the composition, which is assumed to be constant. The product, B, and the byproduct, C, as well as the any residual A are removed at rate F. The coolant, with a heat capacity C_{pc} and an initial temperature of T_{c_0}, is circulated through the heat exchanger shell at rate F_c. T_0 denotes the temperature of the feed f, T denotes the reactor temperature, T_R denotes the temperature of the reaction mass in the tube side of the heat exchanger and T_c denotes the outlet temperature of the cooling medium.

The dynamic model used in this work is derived from Ref. 63, by the following mass and energy balances. The main nominal values for the process parameters are adapted from Ref. 70.

$$\frac{dC_A}{dt} = \frac{F_0}{M}(C_{A_0} - C_A) - k_{10}e^{-\frac{E_{a_1}}{rT}}C_A \tag{4}$$

$$\frac{dC_B}{dt} = -\frac{F_0}{M}C_B + k_{10}e^{-\frac{E_{a_1}}{rT}}C_A - k_{20}e^{-\frac{E_{a_2}}{rT}}C_B \tag{5}$$

$$\frac{dC_C}{dt} = -\frac{F_0}{M}C_C + k_{20}e^{-\frac{E_{a_2}}{rT}}C_B \tag{6}$$

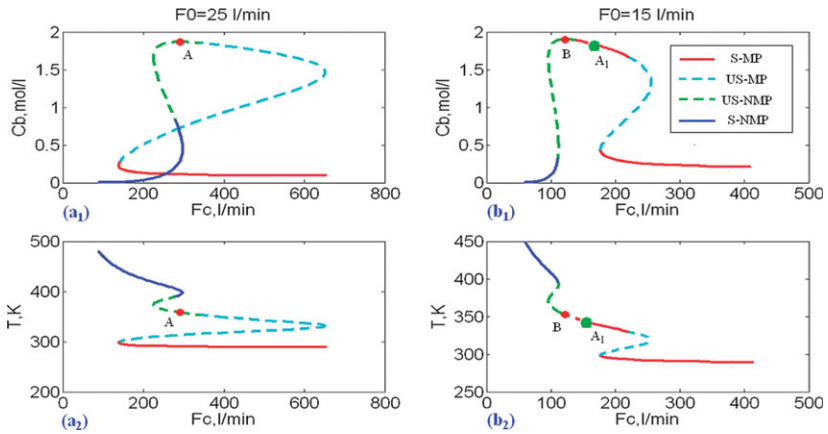

Figure 5. The extended bifurcation diagrams for the reactor-external heat exchanger network (Influences of operating parameter).

[Color figure can be viewed in the online issue, which is available at wileyonlinelibrary.com.]

$$\frac{dT}{dt}=\frac{F_0}{M}(T_0-T)+\frac{R}{M}(T_R-T)-\frac{\Delta H_1}{C_p}k_{10}e^{-\frac{E_{a_1}}{rT}}C_A - \frac{\Delta H_2}{C_p}k_{20}e^{-\frac{E_{a_2}}{rT}}C_B \quad (7)$$

$$\frac{dT_R}{dt}=\frac{R}{M_R}(T-T_R)-\frac{UA}{C_pM_R}(T_R-T_c) \quad (8)$$

$$\frac{dT_C}{dt}=\frac{F_C}{M_C}(T_{C_0}-T_C)+\frac{UA}{C_{pC}M_C}(T_R-T_C) \quad (9)$$

In this case study, a control configuration scheme of $[C_B,T_C]-[F_0,F_C]$ is adopted, whereby $[C_B,T_C]$ is controlled by manipulating $[F_0,F_C]$. Here, we focus on revealing the potential control problems under the given process design, with the chosen control structure. How the operating/design parameters influence the process behavior are analyzed, and then modified to render process design controllable, with the selected control structure in the feasible operating region. In the following process analysis, this "$[C_B,T_C]-[F_0,F_C]$" control structure is referred to as the "base case" design.

Plant-Wide Controllability Analysis. In this section, the control problems associated with the product composition C_B, which are related to the steady-state multiplicities and their effects on the operating/design conditions and phase behavior/stability status, are investigated. Figure 5 shows the steady-state solutions for the plant-wide process, under different operating conditions, for the base case design under the $[C_B,T_C]-[F_0,F_C]$ control configuration. The internal characteristics, including phase behavior and stability/instability status, are presented simultaneously.

From the left section of Figure 5, it can be seen that if the plant-wide process is operated under $F_C\in(176,200)$, the system only exhibits output multiplicity, and has three steady-state solutions. If $F_C\in(203,278)$, the solution diagram exhibits up to five steady-state solutions. With the high-flow rate, F_C, the number of steady-state solutions returns to three. From the right section of Figure 5, the maximum number of steady-state solutions is also three. In the high-profitability operating region, only one unique steady-state solution (point B) is present. Whether $F_0=25$ or $F_0=15$, both input and output multiplicity exist in the solution diagram for the product composition, C_B. It is noteworthy that the whole operating region is segregated into several subregions, which have a different phase behavior and open-loop stability status. The stable-minimum-phase behavior operating region, which is desirable for control system design, is larger when F_0 =15, compared to when F_0 =25. In this case, F_0 accelerates the propagation of nonlinearity. In other words, the feed flow rate, F_0, will affect both the multiplicity behavior and the related stability status.

Similarly, Figure 6 reveals the relationship between the state variables and the manipulated variables under different degrees of reactor holdup, M. The locus in Figure 6 represents the input and output multiplicities between the cooling medium and product composition. However, the reactor temperature only shows output multiplicity, with the behavior of the process being divided into S-MP, US-MP, S-NMP, and US-NMP regions. Figure 6 shows that an increase in the reactor holdup dampens the propagation of the multiplicities, and relieves the burden on the control system design.

As listed in Table 1, $M=1200$, $F_0=25$, and $C_B=1.867$ are the base design/operating parameters. Under this regime, the optimal point (point A) is located in the operating region with unstable-nonminimum-phase behavior and the system is hard to control. As can be seen from Figure 5, the maximum profit (point B) is higher than that under $F_0=25$(point A), however, it still locates in the operating region with unstable-nonminimum-phase behavior. As the designed operating point, where $C_B=1.867$(point A_1), is located in the stable-minimum-phase behavior region when $F_0=15$. Based on the above analysis, decreasing in F_0 could alleviate the control problems with keeping the process economic profit constant, in other words, the higher F_0 has a significant effect on enlarging the size of the unstable-nonminimum-phase regions. The lower F_0 should be preferred.

To convince the effectiveness of the presented framework and to check the above qualitative controllability conclusions, the quantitative controllability at points A, B, and C is also carried out. Based on eigenvalues of the Jacobian matrix, condition numbers (CNs) of points A, B, and A_1 are calculated, the result shows that $CN_{point\,A}>CN_{point\,B}>CN_{point\,A_1}$, lower CN values means that the system exhibits better controllability and should be preferred, state differently, the examined system has the best control performance at point A_1 (Locating in the S-MP region). The

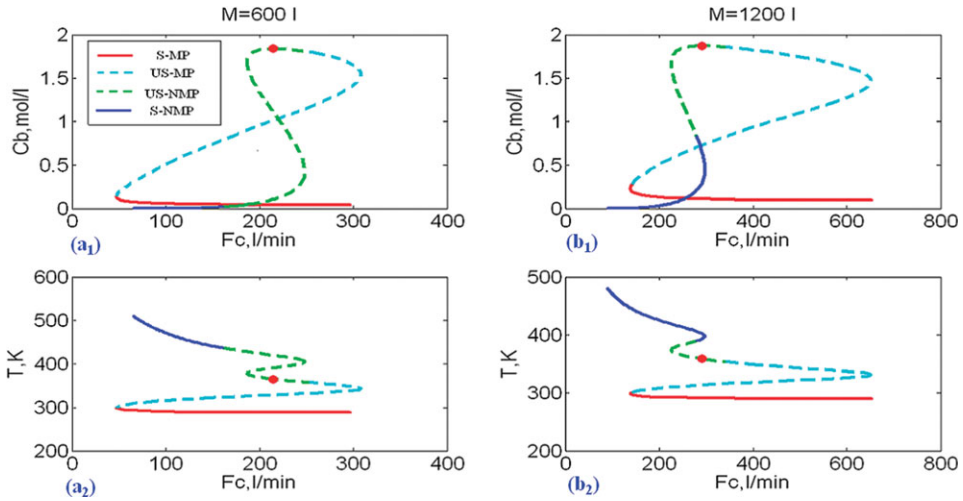

Figure 6. The extended bifurcation diagrams for the reactor-external heat exchanger network (influences of design parameter).

[Color figure can be viewed in the online issue, which is available at wileyonlinelibrary.com.]

results are consistent with results generating from the proposed framework.

According to this reactor-external heat exchanger network, we conclude that any changes to the operating/design conditions may have a profound impact on the nonlinearity/controllability of the process and plant-wide control system design.

Summary. The presented framework for plant-wide process controllability analysis and its resulting suggestions for improving the controllability have been demonstrated with a reactor-external heat exchanger network. It has shown that the multiplicity behavior of the process, under different design/operating conditions; can be evaluated in the parameter domain. When the value of the feed flow rate is large, there are five steady-state solutions under certain operating conditions, but there are only three for lower feed flow rates. A decrease in the inlet feed flow rate may eliminate both the input and output multiplicity behavior to some extent. An increase in the reactor holdup, M, will ameliorate the complexity of the nonlinearity. Both input and output multiplicities are found in the solution diagram for production composition. The reactor temperature has an output multiplicity, but no obvious input multiplicity. The phase behavior and the open-loop stability status are also presented simultaneously. The open-loop stable minimum-phase behavior subregion is smaller with larger feed flow rates. The above results can provide guidance to improve the controllability of the plant-wide process. This case study used a specific set of design/operating parameters, but the lessons can be applied to a wider set of conditions.

Case study II: complex chemical process

In this section, the presented framework will be applied to a complex plant-wide process, to study its controllability from a network perspective.

Process Description. The plant-wide process involves both a reaction system and a separation system.[71] The reaction system occurs in a CSTR, where a first-order exothermic reaction, A+B→P+G, occurs in the liquid phase. The separation system comprises an extract unit, a flash drum unit and a distillation column. Reagent B is fully consumed. The reaction produces a byproduct, G, in addition to the desired product, P. Solvent C is used to extract byproduct G in a single stage extractor. Postextraction, product G is separated out as a purge in the flash drum unit. Solvent C is recycled and made up with fresh solvent-up, to replace the small amount of C lost within the purge. The extractor raffinate can be treated as a binary mixture of A and P. The binary mixture is passed through the distillation column, which contains 10 equilibrium stages, to separate product P from reactant A, which is subsequently returned to the CSTR. The vapor coming from the top of the column is used to preheat the fresh A feed, before any condensation in the condenser unit. The flow sheet for this reaction-separation plant-wide process is depicted in Figure 7.

Modeling Development. Based on the mass and energy balances for the reactor, the extractor, the flash drum unit, the distillation column, and the preheater, a dynamic model for the reactor/separation process has been previously developed.[71] According to the outlined objectives for this study and model's assumptions,[72] the models have been revised to Eqs. 10–33. Table 2 lists the parameters and values for the base design. Note that K_i are computed assuming ideality in the vapor and liquid phase; that is, Raoult's Law applies.

Reactor model

$$V_R \frac{dx_{A_3}}{dt} = F_4 x_{A_4} - F_3 x_{A_3} - V_R x_{A_3} k_0 e^{-E/RT_R} \qquad (10)$$

Table 1. Effects of Design/Operating Parameters on the Maximum of C_B

Design Parameter				Operating Parameter			
M (l)	600	900	**1200**	F_0 (l/min)	5	15	**25**
T (K)	364.5	360.4	**358.43**	T (K)	343.3	353.4	**358.43**
C_B (mol/l)	1.8350	1.8546	**1.8673**	C_B (mol/l)	1.9207	1.8872	**1.8673**

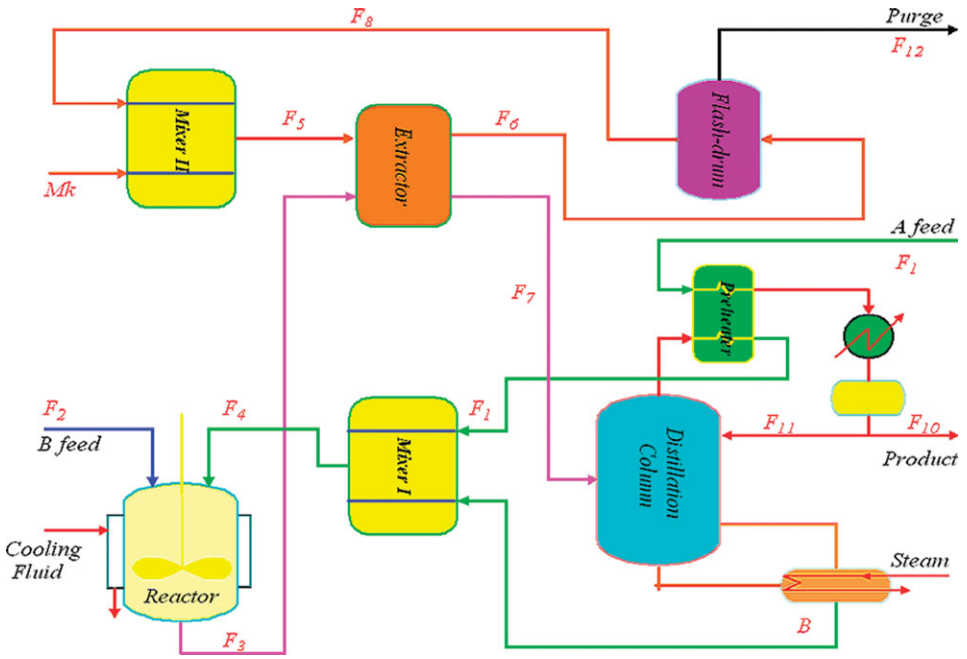

Figure 7. Flow sheet for the reactor-separation plant-wide process.

[Color figure can be viewed in the online issue, which is available at wileyonlinelibrary.com.]

$$V_R \frac{dx_{P_3}}{dt} = -F_3 x_{P_3} + V_R x_{A_3} k_0 e^{-E/RT_R} \tag{11}$$

$$\frac{dT_R}{dt} = \frac{F_4}{V_R} T_4 + \frac{F_2}{V_R} T_2 - \frac{F_3}{V_R} T_R - \frac{\Delta H_R}{M_R C_p} k_0 x_{A_3} e^{-E/RT_R} + \frac{UA_H}{V_R M_R C_p} (T_J - T_R) \tag{12}$$

$$\frac{dT_J}{dt} = \frac{S}{V_J} (T_{J_0} - T_J) - \frac{UA_H}{C_s \rho_s V_J} (T_J - T_R) \tag{13}$$

Extractor model

$$M_E \frac{dx_{G_7}}{dt} = F_3 (x_{G_3} - x_{G_7}) + F_8 x_{G_8} - m(F_8 + Mk) x_{G_7} \tag{14}$$

$$M_E \frac{dx_{A_7}}{dt} = F_3 (x_{A_3} - x_{A_7}) \tag{15}$$

Distillation column model

$$M_D \frac{dx_D}{dt} = VK_2 x_2 - (L + D) x_D \tag{16}$$

$$M \frac{dx_2}{dt} = V(K_3 x_3 - K_2 x_2) + L(x_1 - x_2) \tag{17}$$

$$M \frac{dx_3}{dt} = V(K_4 x_4 - K_3 x_3) + L(x_2 - x_3) \tag{18}$$

$$M \frac{dx_4}{dt} = V(K_5 x_5 - K_4 x_4) + L(x_3 - x_4) \tag{19}$$

$$M \frac{dx_5}{dt} = V(K_6 x_6 - K_5 x_5) + Lx_4 - (L + F_7) x_5 + F_7 (1 - x_{A_7} - x_{G_7}) \tag{20}$$

$$M \frac{dx_6}{dt} = V(K_7 x_7 - K_6 x_6) + (L + F_7)(x_5 - x_6) \tag{21}$$

$$M \frac{dx_7}{dt} = V(K_8 x_8 - K_7 x_7) + (L + F_7)(x_6 - x_7) \tag{22}$$

$$M \frac{dx_8}{dt} = V(K_9 x_9 - K_8 x_8) + (L + F_7)(x_7 - x_8) \tag{23}$$

$$M \frac{dx_9}{dt} = V(K_{10} x_{10} - K_9 x_9) + (L + F_7)(x_8 - x_9) \tag{24}$$

$$M_B \frac{dx_B}{dt} = (L + F_7) x_9 - K_{10} V x_B - B x_B \tag{25}$$

Flash drum model

$$\frac{dP}{dt} = \frac{F_6 RT_f}{V_v} - \frac{F_8 RT_f}{V_v} - \frac{F_{12} P}{V_v} \tag{26}$$

$$M_L \frac{dx_{G_8}}{dt} = F_6 x_{G_6} - \left(\frac{P}{RT_f} F_{12} K_G + F_8 \right) x_{G_8} \tag{27}$$

Preheater model

$$\frac{dT_1}{dt} = \frac{F_1}{V_P} (T_{F_0} - T_1) + \frac{V \Delta H}{V_P C_F} \tag{28}$$

Table 2. Parameters and Values for the Base Design

$F_1 = 50$ kmol/h	$m = 3.995$	$\Delta H = 30$ kJ/kmol
$F_2 = 50$ kmol/h	$M_D = 10$ kmol	$V_P = 5.0075$ kmol
$L = 570$ kmol/h	$M_B = 10$ kmol	$C_F = 32$ kJ/kmol.K
$V = 600$ kmol/h	$T_f = 323.67$ K	$\rho_s = 0.9$ kg/m^3
$V_R = 75$ kmol	$T_4 = 353.5$ K	$\Delta H_R = 87447.58$ kJ/kmol
$V_J = 2.5$ m^3	$T_B = 338.16$ K	$U = 720$ kJ/m^2.K.h
$V_v = 100$ kmol	$T_{J_0} = 553.15$ K	$R = 8.314$ kJ/kmol.K
$M_L = 10$ kmol	$T_{F_0} = 323.67$ K	$S = 4588.294$ m^3/h
$M_E = 2.5$ kmol	$A_H = 25$ m^2	$M_R = 89.36$ kg/kmol
$M = 2.5$ kmol	$C_S = 2.56$ kJ/kg.K	$C_P = 0.34$ kJ/kg.K
$E = 114{,}550$ kJ/kmol	$k_0 = 2.7398 \times 10^{18}$ h^{-1}	$F_{12} = 282.84$ kmol/h

Table 3. Variables for the Reaction-Separation Plant-Wide Process

Controlled Variables	Manipulated Variables
Jacket temperature T_J	Cooling medium flow rate S
Raffinate composition x_{G_7}	Makeup flow rate Mk
Product composition x_D	Reflux flow rate L
Bottom composition x_B	Boil-up rate V
Flash drum pressure P	Purge flow rate F_{12}

Mixer I model

$$F_4 = B + F_1 \tag{29}$$

$$F_4 x_{A_4} = B(1 - x_B) + F_1 \tag{30}$$

$$F_4 T_4 = F_1 T_1 + B T_B \tag{31}$$

Mixer II model

$$F_5 = Mk + F_8 \tag{32}$$

$$F x_{C_5} = F_8(1 - x_{G_8}) + Mk \tag{33}$$

Zero Dynamics Determination. The five controlled variables and five manipulated variables for this case study are shown in Table 3. Based on these variables, zero dynamics will be exhibited.

Set

$$\eta = [\eta_1 \ \eta_2 \ \eta_3 \ \eta_4 \ \eta_5 \ \eta_6 \ \eta_7 \ \eta_8 \ \eta_9 \ \eta_{10} \ \eta_{11} \ \eta_{12} \ \eta_{13} \ \eta_{14}]^T = [x_{A_3} \ x_{P_3} \ T_R \ x_{A_7} \ x_2 \ x_3 \ x_4 \ x_5 \ x_6 \ x_7 \ x_8 \ x_9 \ x_{G_8} \ T_1]^T \tag{34}$$

$$y_{sp} = [y_{sp_1} \ y_{sp_2} \ y_{sp_3} \ y_{sp_4} \ y_{sp_5}]^T = [T_J \ x_{G_7} \ x_D \ x_B \ P]^T \tag{35}$$

After transforming the original plant-wide nonlinear process into the new coordinates, and by applying the algorithm to obtain the zero dynamics for nonlinear systems, the zero dynamics are extracted and expressed as Eqs. A1–A14 (Appendix).

Plant-Wide Controllability Analysis. The steady-state solution diagrams for the reactor–separator–recycle plant-wide process are shown in Figure 8. The composition of A in the reactor product x_{A_3}, the reactor temperature T_R, the jacket temperature T_J, and the product composition x_D are plotted as a function of the cooling medium flow rate.

From Figure 8, the process exhibits multiplicity in the region for the flow rate of the cooling medium, S. The reactor product composition, x_{A_3}, the reactor temperature, T_R, and the product composition, x_D, exhibit output multiplicity. The jacket temperature T_J exhibits both input and output multiplicity. The steady-state curve is similar to that for the single reactor. The upper and lower solutions are stable, but the middle steady state is unstable. The zero dynamics for the original plant-wide process are stable at the lower product composition, and the plant-wide process exhibits nonminimum-phase behavior with unstable zero dynamics. Holding the other four manipulated variables constant, in the cooling medium flow rate space, the entire feasible operating region can be segregated into a stable-minimum-phase behavior subzone, a stable-nonminimum-phase subzone, and an unstable-nonminimum subzone. An unstable-minimum-phase subzone does not exist.

No mathematical model for the chemical plant-wide process can provide a perfect description of the reality, so it is important to analyze the influences of model uncertainties on the nonlinearity and phase behavior. In this case study, the activation energy, E, is selected as the factor of model uncertainty. Its influences on the inherent properties of the plant-wide process are illustrated in Figure 8. Figure 8 reveals the effects of a $\pm 8\%$ change in reaction activation energy, E (E = 114,550), on the phase behavior and open-loop stability status for the process. It suggests that an increase in reaction activation energy, E, can dampen the propagation of the unstable-nonminimum-phase behavior operating subregion, but can accelerate the input multiplicity of jacket temperature.

This base design operating point values are $x_D = 0.861$ with E = 114,550, represented by point B in Figure 8. This point is located at the margin between the stable-

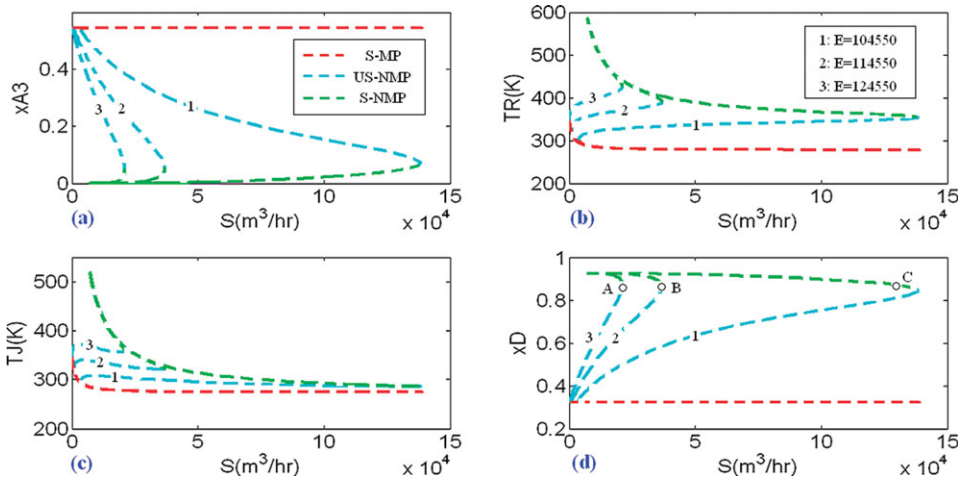

Figure 8. Extended bifurcation diagrams for the plant-wide process under different activation energy.

[Color figure can be viewed in the online issue, which is available at wileyonlinelibrary.com.]

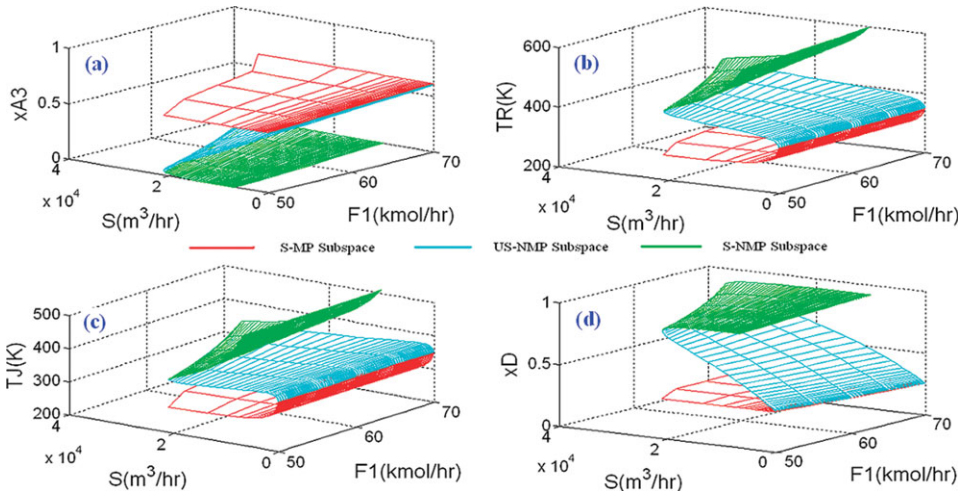

Figure 9. Extended bifurcation diagrams for the plant-wide process (adjustable parameters: feed flow rate F_1 and coolant medium flow rate S).

[Color figure can be viewed in the online issue, which is available at wileyonlinelibrary.com.]

nonminimum-phase behavior and unstable-nonminimum-phase behavior operating subregions. If the reaction activation energy, $E = 124{,}550$, the operating point moves into the unstable-nonminimum-phase behavior subregion. When $E = 104{,}550$, the operating point is in the stable-minimum-phase behavior subregion, at the cost of having higher-coolant medium flow rate. Clearly, a decrease in reaction activation energy will significantly adjust the nonminimum-phase behavior away from the operating point. In line with the above discussion, controlling the plant-wide process at the operating point that provides optimum profit may become increasingly difficult with increasing reaction activation energy. Therefore, it is of critical importance to analyze the influences model uncertainties on the controllability.

The relationship between model uncertainty and controllability for the plant-wide process has been studied, with respect to the reaction activation energy. Simultaneously, changing the feed flow rate, F_1 and the coolant medium flow rate, S was then considered. The maps are depicted in Figure 9, along with the segregation of operation space into subspaces, which exhibit different phase behavior and open-loop stability status. The stable-minimum-phase behavior subspace, the stable-nonminimum-phase behavior subspace, and the unstable-nonminimum-phase behavior subspace exist in the operating space. For the different types of subspace, the nonlinear dynamic behavior may vary.[27] Even a minor disturbance to the unstable-nonminimum-phase behavior operating subspace can lead to an uncontrollable process. Thus, eliminating or avoiding the open-loop unstable-nonminimum-phase behavior subspace could be achieved by adjusting the operating conditions, such as inlet feed flow rate or coolant medium flow rate.

The steady-state solution spaces are presented in Figure 10, where the composition of A in the reactor product x_{A_3}, the reactor temperature T_R, the jacket temperature T_J, and the product composition x_D are plotted as a function of the cooling medium flow rate and boil-up rate. The entire space is segregated into a stable-minimum-phase subspace, a stable-nonminimum-phase subspace, and an unstable-nonminimum-phase subspace. In many cases, operating in an unstable-nonminimum-phase behavior subspace or an unstable-minimum-phase behavior subspace can be more profitable than that in a stable-minimum-phase behavior subspace. In such a scenario, control system design can be challenging. To prevent an undesirable operating subregion with poor controllability and unacceptable dynamic behavior, it is important to identify these inherent properties and improve the dynamic performance at the conceptual design stage. This can be achieved by adjusting the design/operating parameters.

Summary. The phase behavior and open-loop stability status for the plant-wide process have been analyzed using the presented framework. The influences of model uncertainties on these two inherent characteristics have also been investigated. The steady-state spaces for the state variables vs. two manipulated variables have been probed to illustrate how the manipulated variables can affect the behavior of the plant-wide process. The above results can provide a guide for process redesign, by avoiding operations in undesirable subspaces and by enhancing plant-wide control system design.

Conclusions and Future Directions

The steady-state and dynamic behaviors for plant-wide processes with recycles are often substantially different from those for the individual units. Having control of the individual units does not guarantee an effective and smooth running plant-wide control structure. This study has been focused on the controllability analysis of entire chemical process from a network perspective. The presented methodology has been applied to a reactor-external heat exchanger network and a reactor-separator-recycle plant-wide process. The steady-state behaviors for these two plant-wide processes have been studied, and how the open-loop stability status and phase behavior can vary with the manipulated variables has been demonstrated. The entire operating region can be divided into several subregions that possess a different phase behavior and open-loop stability status. The contributions and future directions, based on the presented work, can be summarized as follows:

1. Different manipulated variables impose different influences on the phase behavior and open-loop stability status of an entire plant-wide process. It is important to identify these inherent properties over the entire operating region in the early design stage.

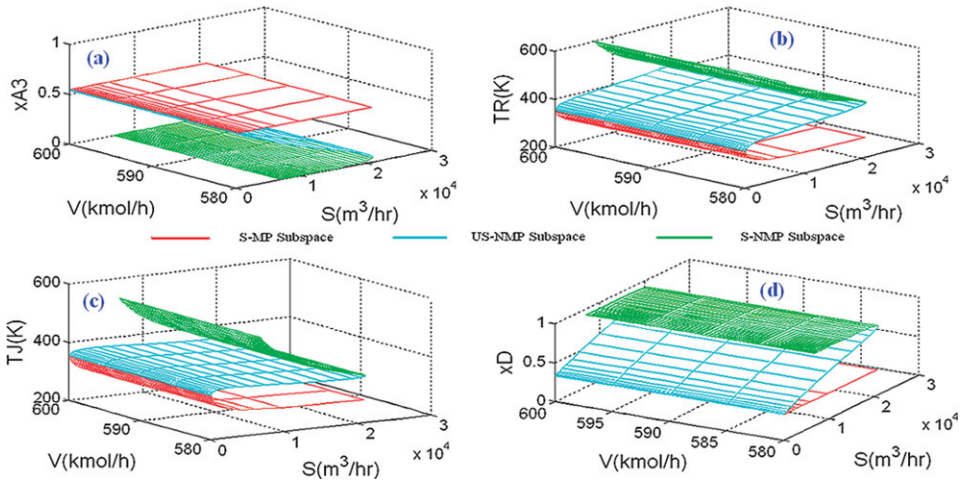

Figure 10. Extended bifurcation diagrams for the plant-wide process (adjustable parameters: boil-up rate *V* and coolant medium flow rate, *S*).

[Color figure can be viewed in the online issue, which is available at wileyonlinelibrary.com.]

2. Profitability is the key objective for management and shareholders in selecting optimal designs. Improving controllability (avoiding nonminimum-phase behavior and open-loop unstable characteristics) may decrease the process economic profit as shown in Figure 5. From the process systems engineering point of view, trade-offs between these two objectives should be made and will give rise to a multiobjective optimization problem.

3. As no mathematical model can provide an accurate prediction of the reality, model uncertainties can impose significant influences on the phase behavior and open-loop stability. As illustrated in Figure 8, the operating point may change with different values of reaction activation energy, E, the variable selected as the factor of model uncertainty. In practice, operating at the margin point can be dangerous, as changes to the operating conditions can lead to steady state and dynamic behaviors that are different from those expected. The influence of model uncertainties on plant-wide controllability needs to be analyzed.

4. The systematic methodology presented in this study allows one to effectively analyze the effects different parameters, such as inputs, disturbances, and design variables, as well as model uncertainties, have on the phase behavior and open-loop stability. Both of these outputs are indicators of open-loop controllability. The results of the analysis provide guidance for the adjustment of design and operation parameters, to eliminate undesirable behaviors in the operating regions. The proposed methodology can also probe the influences of control structure selection on plant-wide controllability, over the entire feasible operating region.

5. It is difficult to characterize the relationship between the complexity of nonlinearity and the structure of the plant-wide process flow sheet. For example, case study I has only two individual units: a reactor and a heat exchanger, whereas case study II is more complex, being made up of seven individual units. With the base design, the nonlinearity in case study I is more complex than that in the latter. Therefore, the steady state behavior for the plant-wide process depends heavily on the mode of operation and the selected design/operating parameters.

6. Operating regions featuring operability problems may be highly profitable operating regions. Many operability problems can be handled by model predictive controllers, however, it is important and valuable to set up the systematic controllability analysis for a chemical process which can fully identify potential operability problems associated with complex behaviors and assess how easy the design is to control at the design stage.

7. Although the case studies only involve a reactor-external heat exchanger network and a reactor–separator–recycle plant-wide process, the proposed approach could also be applied to novel and more complex chemical plant-wide processes, such as continuous bioethanol production processes and biorefinery processes.

8. There are many topological structure alternatives for a plant-wide process at the design stage. In the presented work, the inherent characteristics are investigated under a fixed topology structure. Further research will be undertaken to consider the influence process system topology structure on the phase behavior and open-loop stability. These can be formulated as a large scale stochastic disjunctive mixed-integer nonlinear programming problem which is presently quite difficult to handle. Hence, a robust and efficient algorithm for solving the above problem will further to be studied. By solving the MINLP, a suitable topological structure, having desirable profitability and good controllability over a wide operating region, can be selected.

9. During the last decades, many strategies and their relevant numerical solving frameworks have been presented to tackle the process design/operating parameters decision, control structure selection, and control performance (dynamic operability) simultaneously,[73,74] and the problem can be formulated as a mixed integer dynamic optimization problem, however, the dynamic optimization based approaches presently cannot be applied to large scale chemical process due to computationally demanding even when meet a small number of process units. So, more efficient and robust solving algorithms should be developed in the future. The presented framework for entire chemical process controllability analysis may give guidance for the dynamic optimization-based simultaneous design and control to some extend.

Acknowledgments

The authors gratefully acknowledge financial support from the National Basic Research Program of China (973 Program, Grant No. 2012CB720500) and the Doctoral Fund of Ministry of Education of China (Grant No. 20100002110021).

Notation

Variables: Methodology Framework

F = vector of residuals of the steady-state equations for the process
F_{zd} = vector of residuals of the zero dynamics equations
J_F = Jacobian matrix of F
$J_{F_{zd}}$ = Jacobian matrix of F_{zd}
r_i = relative order of output with respect to the manipulated input
u = manipulated input
x = state variables
y = controlled outputs
α = number of the equations of the zero dynamics

Variables: Reactor-Heat Exchanger Network

C_{A_0} = composition
C_B = product composition
C_{pc} = heat capacity
E_{a_1}, E_{a_2} = activation energies
F_0 = feed flow rate
F_c = coolant flow rate
k_{10}, k_{20} = pre-exponential factors
M = reactor holdup
M_R = holdup in the tube side
T = reactor temperature
T_0 = feed temperature
T_{c_0} = initial temperature
T_c = outlet temperature
T_R = reaction mass temperature
ΔH_1, ΔH_2 = heats of reaction

Variables: Complex Chemical Plant-Wide Process

A_H = heat-transfer area
B = bottom flow rate
C_F = capacity of the feed
C_p = product heat capacity
C_s = steam heat capacity
E = activation energy
F_1 = A feed flow rate
F_2 = B feed flow rate
F_8 = recycle flash flow rate
F_{12} = purge flow rate
k_0 = pre-exponential factor
L = reflux flow rate
m = fraction of the extract and the raffinate compositions
M = holdup in each tray
M_B = holdup in the reboiler
M_D = holdup in the reflux drum
M_E = extractor holdup
M_L = liquid holdup
M_R = molecular weight of product
Mk = makeup flow rate
P = flash drum pressure
R = gas constant
S = cooling medium flow rate
T_{F_0} = A feed temperature
T_2 = B feed temperature
T_{J_0} = steam temperature
T_J = jacket temperature
T_B = bottoms temperature
T_f = flash temperature
T_R = reactor temperature
U = overall heat transfer
V = boil-up rate
V_p = volume of feed in preheater
V_R = reactor volume
V_J = jacket volume
V_v = vapor volume
x_B = bottom composition
x_D = product composition
x_F = A feed composition
x_{G_7} = raffinate composition
ΔH = heat enthalpy of the vapor
ρ_s = steam density
λ = heats of reaction

Literature Cited

1. Morud J, Skogestad S. Effects of recycle on dynamics and control of chemical processing plants. *Comput Chem Eng*. 1996;20:S883–S888.
2. Yuan ZH, Chen BZ, Zhao JS. Effect of manipulated variables selection on the controllability of chemical processes. *Ind Eng Chem Res*. 2011;50:7403–7413.
3. Kumar A, Daoutidis P. Nonlinear dynamics and control of process systems with recycles. *J Process Control*. 2002;12:475–484.
4. Zeyer KP, Pushpavanam S, Kienle A. Nonlinear behavior of reactor-separator networks: influence of separator control structure. *Ind Eng Chem Res*. 2003;42:3294–3303.
5. Yuan ZH, Chen BZ, Zhao JS. Controllability analysis for the liquid-phase catalytic oxidation of toluene to benzoic acid. *Chem Eng Sci*. 2011;66:5137–5147.
6. Uppal A, Ray WH, Poore AB. On the dynamic behavior of continuous stirred tank reactors. *Chem Eng Sci*. 1974;29:967–985.
7. Seider WD, Brengel DD, Widagdo S. Nonlinear-analysis in process design. *AIChE J*. 1991;37:1–38.
8. Russo LP, Bequette BW. Impact of process design on the multiplicity behavior of a jacketed exothermic CSTR. *AIChE J*. 1995;41:135–147.
9. Ray WH, Villa CM. Nonlinear dynamics found in polymerization processes. *Chem Eng Sci*. 2000;55:275–290.
10. Dorn C, Morari M. Qualitative analysis for homogeneous azeotropic distillation. 2. Bifurcation analysis. *Ind Eng Chem Res*. 2002;41:3943–3962.
11. Marquardt W, Monnigmann M. Constructive nonlinear dynamics in process systems engineering. *Comput Chem Eng*. 2005;29:1265–1275.
12. Ramzan N, Faheem M, Gani R. Multiple steady states detection in a packed-bed reactive distillation column using bifurcation analysis. *Comput Chem Eng*. 2010;34:460–466.
13. Silva-Beard A, Flores-Tlacuahuac A. Effect of process design/operation on the steady-state operation on the steady-state operability of a methyl methacrylate polymerization reactor. *Ind Eng Chem Res*. 1999;38:4790–4804.
14. Lopez-Negrete R, Lopez-Rubio J, Flores-Tlacuahuac A. Steady-state multiplicity behavior analysis of a high-impact polystyrene continuous stirred tank reactor using a bifunctional initiator. *Ind Eng Chem Res*. 2006;45:1689–1707.
15. Zavala-Tejeda V, Flores-Tlacuahuac A. The bifurcation behavior of a polyurethane continuous stirred tank reactor. *Chem Eng Sci*. 2006;61:7368–7385.
16. Flores-Tlacuahuac A, Zavala-Tejeda V. Complex nonlinear behavior in the full-scale high-impact polystyrene process. *Ind Eng Chem Res*. 2005;44:2802–2814.
17. Hernjak N, Doyle FJ III, Ogunnaike BA, Pearson RK. *Chemical process characterization for control design*. In: Seferlis P, Georgiadis MC, editors. *The Integration of Process Design and Control, Computer-Aided Chemical Engineering*, Vol. 17. Amsterdam: Elsevier BV, 2004:42–75, Chapter A2.
18. Pushpavanam S, Kienle A. Nonlinear behavior of an ideal reactor separator network with mass recycle. *Chem Eng Sci*. 2001;56:2837–2849.
19. Painuly A, Pushpavanam S, Kienle A. Steady state behavior of coupled nonlinear reactor-separator systems: effect of different separators. *Ind Eng Chem Res*. 2005;44:2165–2173.
20. Kiss AA, Bildea CS, Dimian AC, Iedema PD. State multiplicity in CSTR-separator-recycle polymerization systems. *Chem Eng Sci*. 2002;57:535–546.
21. Bildea CS, Dimian AC, Iedema PD. Nonlinear behavior of reactor separator recycle systems. *Comput Chem Eng*. 2000;24:209–214.
22. Yuan ZH, Chen BZ, Zhao JS. An overview on controllability analysis of chemical processes. *AIChE J*. 2011;57:1185–1201.

23. Morari M. Effect of design on the controllability of chemical plants, In: Proc. IFAC Workshop on Interactions between Process Design and Process Control, London, International Federation of Automatic Control, 1992.
24. Hahn J, Monnigmann M, Marquardt W. A method for robustness analysis of controlled nonlinear systems. *Chem Eng Sci*. 2004;59:4325–4338.
25. Hahn J, Martin M, Marquardt W. On the use of bifurcation analysis for robust controller tuning for nonlinear systems. *J Process Control*. 2008;18:408–420.
26. Ma K, Bogle D. Process design in SISO systems with input multiplicity using bifurcation analysis and optimisation. *J Process Control*. 2010;20:241–247.
27. Yuan ZH, Wang HZ, Chen BZ, Zhao JS. Operating zone segregation of chemical reaction systems based on stability and nonminimum phase behavior analysis. *Chem Eng J*. 2009;155:304–311.
28. Luyben WL. *Plant-Wide Control*. New York: McGraw-Hill, 1999.
29. Kaymak DB, Luyben WL. Evaluation of a two-temperature control structure for a two-reactant two-product type of reactive distillation column. *Chem Eng Sci*. 2006;61:4432–4450.
30. McAvoy TJ. Synthesis of plant-wide control systems using optimization. *Ind Eng Chem Res*. 1999;38:2984–2994.
31. Wang P, McAvoy TJ. Synthesis of plant-wide control systems using a dynamic model and optimization. *Ind Eng Chem Res*. 2001;40:5732–5742.
32. Skogestad S. Plantwide control: the search for the self-optimizing control structure. *J Process Control*. 2000;10:487–507.
33. Stephanopoulos G, Ng C. Perspectives on the synthesis of plant-wide control structure. *J Process Control*. 2000;10:97–111.
34. Skogestad S. Control structure design for complete chemical plants. *Comput Chem Eng*. 2004;28:219–234.
35. Cao Y, Yang Z. Multiobjective process controllability analysis. *Comput Chem Eng*. 2004;28:83–90.
36. Ricardez-Sandoval LA, Douglas PL. A methodology for the simultaneous design and control of large-scale systems under process parameter uncertainty. *Comput Chem Eng*. 2011;35:307–318.
37. Ricardez-Sandoval LA, Douglas PL. Simultaneous design and control of chemical processes with application to the Tennessee Eastman process. *J Process Control*. 2009;19:1377–1391.
38. Ricardez-Sandoval LA, Douglas PL. Integration of design and control for chemical processes: a review of the literature and some recent results. *Annu Rev Control*. 2009;33:158–171.
39. Rojas OJ, Setiawan R, Bao J. Dynamic operability analysis of nonlinear process networks based on dissipativity. *AIChE J*. 2009;55:963–982.
40. Scattolini R. Architectures for distributed and hierarchical model predictive control—a review. *J Process Control*. 2009;19:723–731.
41. Araujo A, Skogestad S. Control structure design for the ammonia synthesis process. *Comput Chem Eng*. 2008;32:2920–2932.
42. Baldea M, Araujo A, Skogestad S. Dynamic considerations in the synthesis of self-optimizing control structures. *AIChE J*. 2008;54:1830–1841.
43. Vasudevan S, Rangaiah GP, Konda NV, Tay WH. Application and evaluation of three methodologies for plant-wide control of the styrene monomer plant. *Ind Eng Chem Res*. 2009;48:10941–10961.
44. Sun Y, El-Farra NH. Quasi-decentralized model-based networked control of process systems. *Comput Chem Eng*. 2008;32:2016–2029.
45. Rawling JR, Stewart BT. Coordinating multiple optimization-based controllers: new opportunities and challenges. *J Process Control*. 2008;18:839–845.
46. Liu JF, Christofides PD. Distributed model predictive control of nonlinear systems subject to asynchronous and delayed measurements. *Automatica* 2010;46:52–61.
47. Liu JF, Christofides PD. Distributed model predictive control of nonlinear systems. *AIChE J*. 2009;55:1171–1184.
48. Xu S, Bao J. Distributed control of plantwide chemical processes. *J Process Control*. 2009;19:1671–1687.
49. Biegler LT, Zavala VM. Large-scale nonlinear programming using IPOPT. *Comput Chem Eng*. 2009;33:575–582.
50. Ochoa S, Repke JU, Wozny G. Integrating real-time optimization and control for optimal operation: application to the bioethanol process. *Biochem Eng J*. 2010;53:18–25.
51. Ochoa S, Wozny G, Repke JU. Plantwide optimizing control of a continuous bioethanol production process. *J Process Control*. 2010;20:983–998.
52. Zavala VM, Biegler LT. Fast implementations and rigorous models: can both be accommodated in NMPC? *Int J Robust Nonlinear Control*. 2007;18:800–815.
53. Engell S. Feedback control for optimal process operation. *J Process Control*. 2007;17:203–219.
54. Manenti F, Rovaglio M. Integrated multilevel optimization in large-scale poly(ethylene terephthalate) plants. *Ind Eng Chem Res*. 2007;47:92–104.
55. Ochoa S. Plantwide optimizing control for the continuous bio-ethanol production process, *Ph.D Thesis, Technischen Universitat Berlin*, Berlin, 2010.
56. Morari M. Design of resilient processing plants-III. A general framework for the assessment of dynamic resilience. *Chem Eng Sci*. 1983;38:1881–1991.
57. Luyben WL. Snowball effects in reactor/separator processes with recycle. *Ind Eng Chem Res*. 1994;33:299–305.
58. Seider WD, Seader JD, Lewin DR. *Product and Process Design Principles: Synthesis, Analysis, and Evaluation*. New York: Wiley, 2004.
59. Meel A, Seider WD. Game theoretic approach to multiobjective designs: focusing on inherent safety. *AIChE J*. 2006;52:228–246.
60. Wang HZ, Yuan ZH, Chen BZ. Analysis of the stability and controllability of chemical processes. *Comput Chem Eng*. 2011;35:1101–1109.
61. Groenendijk S, Plantwide controllability and structural optimization of plants with recycle, *Ph.D Thesis, Universiteit Van Amsterdam*, Netherlands, 2000.
62. Isidori A. *Nonlinear Control Systems*. Berlin: Springer Verlag, 1989.
63. Yuan ZH, Chen BZ, Zhao JS. Phase behavior analysis for industrial polymerization reactors. *AIChE J*. 2011;57:2795–2807.
64. Seider WD, Seader JD, Lewin DR. *Process Design Principles: Synthesis, Analysis, and Evaluation*. New York: Wiley, 1999.
65. McAuley KB, Macdonald DA, Mclellan PJ. Effects of operating conditions on stability of gas-phase polyethylene reactors. *AIChE J*. 1995;41:868–879.
66. Baldea M, Daoutidis P. Model reduction and control of reactor-heat exchanger networks. *J Process Control*. 2006;16:265–274.
67. Dadebo SA, Bell ML, Mclellan PJ, McAuley KB. Temperature control of industrial gas phase polyethylene reactors. *J Process Control*. 1997;7:83–95.
68. Henderson LS, Cornejo RA. Temperature control of continuous, bulk styrene polymerization reactors and the influence of viscosity: an analytical study. *Ind Eng Chem Res*. 1989;28:1644–1653.
69. Baldea M, Daoutidis P. Modelling, dynamics and control of process networks with high energy throughput. *Comput Chem Eng*. 2008;32:1964–1983.
70. Marrpquin G, Luyben WL. Practical control studies of batch reactors using realistic mathematical models. *Chem Eng Sci*. 1973;28:993–1003.
71. Samyudia Y. Control of multi unit processing plants, Ph.D Thesis, The University of Queensland, Australia, 1995.
72. Lee PT, Li HZ, Cameron IT. Decentralized control design for nonlinear multi-unit plants: a gap metric approach. *Chem Eng Sci*. 2000;55:3743–3758.
73. Bansal V, Perkins JD, Pistikopoulos EN. A case study in simultaneous design and control using rigorous, mixed-integer dynamic optimization models. *Ind Eng Chem Res*. 2002;41:760–778.
74. Sakizlis V, Perkins JD, Pistikopoulos EN. Recent advances in optimization-based simultaneous process and control design. *Comput Chem Eng*. 2004;28:2069–2086.

Appendix

This appendix describes the zero dynamics of the reactor–separator–recycle plant-wide process. Based on the detailed algorithm listed in, zero dynamics will be obtained as follow.

$$\dot{\eta}_1 = \left[(B(1-y_{sp_4}) + F_1 - (F_1+F_2+B)\eta_1 - V_R\eta_1 k_0 \exp(-E/R/\eta_3))/V_R\right] \tag{A1}$$

$$\dot{\eta}_2 = \left[(-(F_1+F_2+B)\eta_2 + V_R\eta_1 k_0 \exp(-E/R/\eta_3))/V_R\right] \tag{A2}$$

$$\dot{\eta}_3 = \begin{bmatrix} (F_1\eta_{14} + BT_B)/V_R + F_2T_2/V_R - \Delta H_R k_0 \exp(-E/R/\eta_3)/M_R/C_p\eta_1 \\ -(F_1+F_2+B)\eta_3/V_R + UA_H(y_{sp_1} - \eta_3)\eta_3/V_R/M_R/C_p \end{bmatrix} \tag{A3}$$

$$\dot{\eta}_4 = \left[(F_1+F_2+B)(\eta_1 - \eta_4)/M_E\right] \tag{A4}$$

$$\dot{\eta}_5 = \begin{bmatrix} (By_{sp_3}y_{sp_4} + D\eta_{12}y_{sp_3} - (F_1+B+F_2)\eta_{12}y_{sp_3})/(K_2\eta_5\eta_{12} - K_{10}y_{sp_3}y_{sp_4}) \\ (K_3\eta_6 - K_2\eta_5) + ((K_{10}(By_{sp_3}y_{sp_4} + D\eta_{12}y_{sp_3} - (F_1+B+F_2)\eta_{12}y_{sp_3})/ \\ (K_2\eta_5\eta_{12} - K_{10}y_{sp_3}y_{sp_4})y_{sp_4} + By_{sp_4}) - (F_1+B+F_2)\eta_{12})/\eta_{12}(y_{sp_3} - \eta_5) \end{bmatrix} \tag{A5}$$

$$\dot{\eta}_6 = \begin{bmatrix} (By_{sp_3}y_{sp_4} + D\eta_{12}y_{sp_3} - (F_1+B+F_2)\eta_{12}y_{sp_3})/(K_2\eta_5\eta_{12} - K_{10}y_{sp_3}y_{sp_4}) \\ (K_4\eta_7 - K_3\eta_6) + ((K_{10}(By_{sp_3}y_{sp_4} + D\eta_{12}y_{sp_3} - (F_1+B+F_2)\eta_{12}y_{sp_3})/ \\ (K_2\eta_5\eta_{12} - K_{10}y_{sp_3}y_{sp_4})y_{sp_4} + By_{sp_4}) - (F_1+B+F_2)\eta_{12})/\eta_{12}(\eta_5 - \eta_6) \end{bmatrix} \tag{A6}$$

$$\dot{\eta}_7 = \begin{bmatrix} (By_{sp_3}y_{sp_4} + D\eta_{12}y_{sp_3} - (F_1+B+F_2)\eta_{12}y_{sp_3})/(K_2\eta_5\eta_{12} - K_{10}y_{sp_3}y_{sp_4}) \\ (K_5\eta_8 - K_4\eta_7) + ((K_{10}(By_{sp_3}y_{sp_4} + D\eta_{12}y_{sp_3} - (F_1+B+F_2)\eta_{12}y_{sp_3})/ \\ (K_2\eta_5\eta_{12} - K_{10}y_{sp_3}y_{sp_4})y_{sp_4} + By_{sp_4}) - (F_1+B+F_2)\eta_{12})/\eta_{12}(\eta_6 - \eta_7) \end{bmatrix} \tag{A7}$$

$$\dot{\eta}_8 = \begin{bmatrix} (By_{sp_3}y_{sp_4} + D\eta_{12}y_{sp_3} - (F_1+B+F_2)\eta_{12}y_{sp_3})/(K_2\eta_5\eta_{12} - K_{10}y_{sp_3}y_{sp_4}) \\ (K_6\eta_9 - K_5\eta_8) + ((K_{10}(By_{sp_3}y_{sp_4} + D\eta_{12}y_{sp_3} - (F_1+B+F_2)\eta_{12}y_{sp_3})/ \\ (K_2\eta_5\eta_{12} - K_{10}y_{sp_3}y_{sp_4})y_{sp_4} + By_{sp_4}) - (F_1+B+F_2)\eta_{12})/\eta_{12}(\eta_7 - \eta_8) \\ -(F_1+B+F_2)\ \eta_8 + (F_1+B+F_2)\ (1 - \eta_4 - y_{sp_2}) \end{bmatrix} \tag{A8}$$

$$\dot{\eta}_9 = \begin{bmatrix} (By_{sp_3}y_{sp_4} + D\eta_{12}y_{sp_3} - (F_1+B+F_2)\eta_{12}y_{sp_3})/(K_2\eta_5\eta_{12} - K_{10}y_{sp_3}y_{sp_4}) \\ (K_7\eta_{10} - K_6\eta_9) + (((K_{10}(By_{sp_3}y_{sp_4} + D\eta_{12}y_{sp_3} - (F_1+B+F_2)\eta_{12}y_{sp_3})/ \\ (K_2\eta_5\eta_{12} - K_{10}y_{sp_3}y_{sp_4})y_{sp_4} + By_{sp_4}) - (F_1+B+F_2)\eta_{12})/\eta_{12} \\ +(F_1+B+F_2))(\eta_8 - \eta_9) \end{bmatrix} \tag{A9}$$

$$\dot{\eta}_{10} = \begin{bmatrix} (By_{sp_3}y_{sp_4} + D\eta_{12}y_{sp_3} - (F_1+B+F_2)\eta_{12}y_{sp_3})/(K_2\eta_5\eta_{12} \\ -K_{10}y_{sp_3}y_{sp_4})(K_8\eta_{11} - K_7\eta_{10}) + (((K_{10}(By_{sp_3}y_{sp_4} + D\eta_{12}y_{sp_3} \\ -(F_1+B+F_2)\eta_{12}y_{sp_3})/(K_2\eta_5\eta_{12} - K_{10}y_{sp_3}y_{sp_4})y_{sp_4} + By_{sp_4}) \\ -(F_1+B+F_2)\eta_{12})/\eta_{12} + (F_1+B+F_2))(\eta_9 - \eta_{10}) \end{bmatrix} \tag{A10}$$

$$\dot{\eta}_{11} = \begin{bmatrix} (By_{sp_3}y_{sp_4} + D\eta_{12}y_{sp_3} - (F_1+B+F_2)\eta_{12}y_{sp_3})/(K_2\eta_5\eta_{12} \\ -K_{10}y_{sp_3}y_{sp_4})(K_9\eta_{12} - K_8\eta_{11}) + (((K_{10}(By_{sp_3}y_{sp_4} + D\eta_{12}y_{sp_3} \\ -(F_1+B+F_2)\eta_{12}y_{sp_3})/(K_2\eta_5\eta_{12} - K_{10}y_{sp_3}y_{sp_4})y_{sp_4} + By_{sp_4}) \\ -(F_1+B+F_2)\eta_{12})/\eta_{12} + (F_1+B+F_2))(\eta_{10} - \eta_{11}) \end{bmatrix} \tag{A11}$$

$$\dot{\eta}_{12} = \begin{bmatrix} (By_{sp_3}y_{sp_4} + D\eta_{12}y_{sp_3} - (F_1+B+F_2)\eta_{12}y_{sp_3})/(K_2\eta_5\eta_{12} \\ -K_{10}y_{sp_3}y_{sp_4})(K_{10}y_{sp_4} - K_9\eta_{12}) + (((K_{10}(By_{sp_3}y_{sp_4} + D\eta_{12}y_{sp_3} \\ -(F_1+B+F_2)\eta_{12}y_{sp_3})/(K_2\eta_5\eta_{12} - K_{10}y_{sp_3}y_{sp_4})y_{sp_4} + By_{sp_4}) \\ -(F_1+B+F_2)\eta_{12})/\eta_{12} + (F_1+B+F_2))(\eta_{11} - \eta_{12}) \end{bmatrix} \tag{A12}$$

$$\dot{\eta}_{13} = \begin{bmatrix} ((F_1+B+F_2)(1 - \eta_1 - \eta_2 - y_{sp_2}) - K\eta_{13}((F_1+B+F_2) \\ (1 - \eta_1 - \eta_2 - y_{sp_2}) + F_8\eta_{13})/m/y_{sp_2})/M_L \end{bmatrix} \tag{A13}$$

$$\dot{\eta}_{14} = \left[F_1(T_{F_0} - \eta_{14})/V_p + (By_{sp_3}y_{sp_4} + D\eta_{12}y_{sp_3} - (F_1+B+F_2)\eta_{12}y_{sp_3})/(K_2\eta_5\eta_{12} - K_{10}y_{sp_3}y_{sp_4})\Delta H/V_p/C_F\right] \tag{A14}$$

Manuscript received Jun. 8, 2011, and revision received Dec. 5, 2011.